Supporting information

A ceramide-regulated element in the late endosomal protein LAPTM4B controls amino acid transporter interaction

Kecheng Zhou[1,2‡], Andrea Dichlberger[1,2‡], Hector Martinez-Seara[3,4], Thomas K.M. Nyholm[5], Shiqian Li[1,2], Young Ah Kim[6], Ilpo Vattulainen[4,7], Elina Ikonen[1,2], Tomas Blom[1,2*]

[1] Department of Anatomy, Faculty of Medicine, University of Helsinki, Helsinki, Finland

[2] Minerva Foundation Institute for Medical Research, Helsinki, Finland

[3] Institute of Organic Chemistry and Biochemistry of the Czech Academy of Sciences, Prague, Czech Republic

[4] Laboratory of Physics, Tampere University of Technology, Tampere, Finland

[5] Biochemistry, Faculty of Science and Engineering, Åbo Akademi University, Turku, Finland

[6] Department of Chemistry and Biochemistry, Queens College, City University of New York, Flushing, NY 11367, USA

[7] Department of Physics, University of Helsinki, Helsinki, Finland

Supporting Information

Materials

Mouse monoclonal anti-Flag (M2) (Sigma-Aldrich, Cat#F1804); CD98 antibody (C-20) (Santa Cruz Biotechnology, Cat#sc-7095); CD98 antibody (E5) (Santa Cruz Biotechnology, Cat#sc-376815); Phospho-p70 S6 Kinase (Thr389) antibody (Cell Signaling, Cat#9205); S6 Kinase (Santa Cruz Biotechnology, Cat#sc-8418); Goat Anti-Mouse IgG (H+L)-HRP conjugate (BIORAD, Cat#1706516); Peroxidase AffiniPure Donkey Anti-Goat IgG (H+L) (Jackson ImmunoResearch, Cat#705-035-147); Goat Anti-Rabbit IgG (H+L)-HRP Conjugate (BIORAD, Cat#1706515); Goat anti-Mouse IgG (H+L) Cross-Adsorbed Secondary Antibody, Alexa Fluor 488 (ThermoFisher Scientific, Cat#A-11001); IRDye 680LT Donkey anti-Goat IgG (H+L) (LI-COR, Cat#925-68024); IRDye 800CW Goat anti-Mouse IgG (H+L) (LI-COR, Cat#925-32210); Anti-Flag M2 affinity gel (Sigma-Aldrich, Cat#A2220); Sphingomyelinase from *Staphylococcus aureus* (Sigma-Aldrich, Cat#S8633); Ceramide-BP-BPY[1]; C6-Ceramide (Enzo, Cat#BML-SL110-0005); C6-Sphingomyelin (Larodan, Cat#56-1083-4); Sphingosine (Enzo, Cat#BML-EI155-0025); C6-Glucosylceramide (Larodan, Cat#56-1049); DTME (ThermoFisher

Scientific, Cat#22335), LC-SPDP (ThermoFisher Scientific, Cat#21651); L-[4,5-3H]-Leucine (PerkinElmer, Cat#NET1166001MC); GFP-Trap®_MA beads (Chromotek, Cat#gtma-20); MEM amino acids (Gibco, Cat#11130-036). Peptides WALP23, LAPTM4B TM1, TM2, and TM3 were custom synthesized by Anaspec and TM4 by Genscript. 1-palmitoyl-2-propionyl [DPH]-sn-glycero-3-phosphocholine (DPH-PC) was obtained from Molecular Probes (Eugene, OR).

Plasmids and siRNAs

LAPTM4B mutants were generated by site-directed mutagenesis PCR using sequence-specific oligos (see Table S11). 3xFlag-tagged CD63 WT, LAPTM4A WT, LAPTM4B WT, and LAPTM4B mutant inserts were cloned into pEFIRES-P plasmid via Eco*RI* and Xba*I* sites [2] (kindly provided by Dr. Olli Ritvos). Cherry-tagged LAPTM4B was generated as described previously [1]. Constructs for FRET analysis were generated by cloning LAPTM4B WT or CD63 WT into pVenus-N1 plasmids using Xho*I*/Bam*HI* and Bgl*II*/Sal*I* sites, respectively. 4F2hc was amplified by PCR from A431 cDNA and cloned into pCerulean-C1 vector using Xho*I*/Bam*HI* sites. GFP-KDEL was kindly provided by Prof. Eija Jokitalo [3]. The LAMP1-mGFP construct was obtained from Addgene (#34831) and has been originally generated by[4]. Detailed information about all constructs used in the study can be found in Table S11. SiRNAs against human LAPTM4B, SMPD1, and ASAH1 have been described previously [1]. SiRNA against human 4F2hc (SLC3A2; Ambion, Cat#4392420) is AGCUCAUACCUGUCUGAUUTT (sense). All siRNAs were used at a final concentration of 10nM and cells were treated 2-3 days. For siRNA sequence details see Table S13.

Cell culture

A431 cells (ATCC, Cat#CRL-1555) and HeLa cells (ATCC, CAT#CCL-2) were maintained in Dulbecco's modified Eagle's medium containing 10% fetal bovine serum (FBS), penicillin, and streptomycin at 37 °C in 5% CO2. Cells were treated with 50mU/mL bacterial sphingomyelinase (Sigma, CAT#S-8633) for 30 minutes to generate ceramide. To assess mTORC1 activity, cells were starved for 1h with Earle's Balanced Salt Solution (EBSS), and subsequently refed with Stimulation Medium (EBSS:complete medium; 1:1) for different time points.

Generation of knockout cells and stable cell lines

LAPTM4B A431 knockout cells were generated by CRISPR/Cas9-mediated genome engineering as described previously [5,6]. Briefly, coding sequences in exon 3 of LAPTM4B (Gene ID: 55353) were selected and analyzed for the design of Cas9 nickase targets (http://crispr.mit.edu). sgRNA guides were synthesized and subcloned into the sgRNA expression vector using Bbs*I* sites (see Table S11). A431 cells were co-transfected with Cas9 nickase and two matching pairs of the sgRNA expressing plasmids using Lipofectamine LTX with PLUS reagent (Invitrogen, Cat#15338100), and subjected to puromycin (1µg/mL) selection for 48h post-transfection. Cells were further cultured in normal cell culture medium without puromycin for another 4 days. Subsequently, single clones were isolated and finally verified by Sanger sequencing. Cas9 nickase targets with effective knockout efficiency were used for this study and are shown in **Figure S2A and S2B**. As described previously [2], for the generation of stable cell lines, A431 LAPTM4B knockout cells were transfected with pEFIRES-P plasmids containing either CD63 WT, LAPTM4A WT, LAPTM4B WT or mutant LAPTM4B (**see Figure S2C and S2D**) using Lipofectamine LTX with PLUS reagent. Cells were grown in culture medium containing 1µg/mL puromycin until a resistant cell pool was formed. A431 cells stably expressing LAPTM4B WT or CD63 WT were generated as described [1] and were used for Co-IP and MS experiments in this study.

Quantitative PCR

qPCR was performed as described previously [1].

Western blot

Cells were washed with PBS, scraped in SDS boiling buffer (2.5% SDS, 250 mM Tris/HCl pH 6.8, including 50 mM NaF, 10 mM b-glycerophosphate, 0.5 mM DTT, 0.5 mM PMSF), and lysates were boiled at 98^{o}C for 10 minutes. Equal amounts of proteins were resolved on 12% Mini-Protean TGX Stain-Free gels (BioRad Cat#161-0185) and transferred onto LF-PVDF (BIORAD Cat#170-4274) or nitrocellulose membrane (BIORAD Cat#170-4270). Membranes were blocked with 5% milk in TBS containing 0.1% Tween-20 or Odyssey Blocking Buffer (LI-COR; Cat#927-40000) for 1h at room temperature, and subsequently probed with primary antibodies (Anti-Flag M2, 1:1,000 - 1:2,000; anti-CD98 C-20, 1:1,000; Anti-phospho-p70 S6K, 1:1,000 – 1:2,000, Anti-S6K, 1:1,000) at 4 ^{o}C overnight. After washing with TBS containing 0.1% - 0.15% Tween-20, membranes were incubated with secondary antibodies for 45 minutes at room temperature. Membranes were washed, incubated with ECL Clarity (BIORAD, Cat#170-5060) or ECL Clarity Max substrate (BIORAD Cat#170-5062), and imaged with a ChemiDoc Touch Imaging System (BIORAD). For the detection of fluorescently-labeled

antibodies, membranes were scanned with an Odyssey CLX Imaging System (LI-COR). Band intensities were analyzed using either Image Studio Software (LI-COR; version 5.0), Image J software (version 1.50b; https://imagej.nih.gov/ij/), or Image Lab software (version 5.2.1; BIO-RAD) and normalized to total protein content quantified with the Stain-Free technology (BIO-RAD).

Immunoprecipitation

Cells were seeded in 100-mm dishes three days prior to the experiment. Fresh medium was applied to the cells four hours prior crosslinking with 0.4 mM DTME and 0.1 mM LC-SPDP in DPBS (PBS containing 0.5 mM $MgCl_2$ and 0.9 mM $CaCl_2$) for 2 hours at 4 ^oC. Cells were quenched with 20 mM Tris-Cl (pH8.0) and 5 mM DL-cysteine in DPBS for 15 minutes on ice, washed with cold DPBS, and scraped in lysis buffer (25 mM Tris-HCl pH 7.5, 150 mM NaCl, 1% NP-40, 0.1% SDS, 0.5% NaDoc, 1 mM EDTA) containing protease inhibitor cocktail (Sigma, Cat #P8340). Lysates were cleared by centrifugation at 16,000 x g for 10 minutes at 4 ^oC. Equal amounts of cleared cell lysates were incubated with Anti-Flag M2 affinity gel overnight at 4 ^oC. Resins were washed four times with cold lysis buffer, eluted in 2x SDS sample buffer, and incubated for 15 minutes at 65 ^oC. Precipitated proteins were detected by Western blotting as described above.

Immunofluorescence and confocal microscopy

Cells were seeded on glass coverslips and transfected with different plasmids by using Effectene transfection reagent (QIAGEN, Cat#301425) 2-3 days prior to experiments. Cells were fixed in 4% paraformaldehyde in PBS for 20 minutes at room temperature (anti-Flag), or 100% ice-cold methanol for 15 minutes at -20 ^oC (anti-CD98 (E5))) and then quenched with 50 mM NH_4Cl for 10 minutes at room temperature. Cells were washed with PBS and permeabilized with 0.1% Triton X-100 in PBS for 10 minutes at room temperature, blocked in 10% FBS in PBS for 30 minutes, and then incubated with anti-Flag M2 (Sigma, Cat# F1804, 1:400) or anti-CD98 (E5) (Santa Cruz, Cat# sc-346815, 1:200) for 45 minutes at 37 ^oC. Cells were washed in PBS and labeled with secondary antibodies accordingly for 45 minutes at 37 ^oC. Coverslips were washed in PBS, rinsed in H_2Odd and mounted on microscope slides using Mowiol/DABCO (Calbiochem, Cat#475904/Sigma Cat#D-2522). Images were captured with Leica TCS SP8 confocal microscope, and images were analyzed by ImageJ.

Fluorescence Resonance Energy Transfer (FRET)

For FRET analysis, LAPTM4B-Venus, CD63-Venus, and 4F2hc-Cerulean plasmids were cloned and validated by sequencing. A431 cells were prepared for imaging as described in the Method Details

section Immunofluorescene and confocal microscopy. Venus-Linker-Cerulean was used as positive control and the FRET pair CD63-Venus and 4F2hc-Cerulean was used as negative control. FRET was conducted on a Leica TCS CARS SP8 confocal microscope. The acceptor photobleaching method was carried out with the following settings (Donor = Cerulean, excitation 458 nm; emission 462-510 nm; Acceptor = Venus, excitation 514 nm; emission 518-580 nm). FRET efficiency was calculated by Leica Application Suite (Advanced Fluorescence 3.0.0 build 8134), $FRET_{eff} = (D_{post} - D_{pre}) / D_{post}$.

Ceramide-BP-BPY crosslinking

Ceramide-BP-BPY crosslinking was performed as described previously [1]. Briefly, A431 cells stably expressing Flag-tagged WT or mutant LAPTM4B were grown to confluency in 100-mm dishes, and then incubated with 1 µM Ceramide-BP-BPY for 1.5 hours. For the competition experiments, the indicated concentrations of C6-ceramide, C6-sphingomyelin, sphingosine, or C6-glucosylceramide were incubated concomitantly with the crosslinkable ceramide-BP-BPY during the 1.5 hour incubation time prior UV-crosslinking. Cells were placed on ice, washed three times with ice-cold PBS, and Ceramide-BP-BPY was crosslinked for 20 minutes using a Spectrolinker XL-1500 with six UV-A lamps (365 nm). Subsequently, cells were scraped in lysis buffer (50 mM Na_2HPO_4, 0.3 M NaCl, pH to 8.0) containing 0.85 % Triton X-100 and protease inhibitor cocktail. Flag-tagged proteins were immuno-precipitated with anti-FLAG M2 Affinity Gel (Sigma, Cat#A2220) at 4 ^{o}C overnight. Precipitated proteins were resolved by SDS-PAGE and crosslinked Ceramide-BP-BPY was detected by in-gel fluorescence imaging using a FLA9000-imager. Total precipitated protein was further analyzed by Western blotting as described.

Equilibrium distribution of ceramide-BODIPY between donor and acceptor vesicles

The distribution of ceramide-BODIPY (N-palmitoyl-D-erythro-sphingosine-BODIPY, [7]) between large unilamellar donor vesicles (donor LUVs) and large unilamellar acceptor vesicles (acceptor LUVs) was studied by a FRET approach, in which the FRET donor was DPH-PC and the FRET acceptor ceramide-BODIPY (method modified from [8]). Donor LUVs were prepared from 100 nmol phospholipid POPC (Avanti, Cat#850457P) and 0.5 mol% DPH-PC and 0.5 mol% ceramide-BODIPY. Acceptor vesicles were prepared from 100 nmol phospholipids with or without 2 mol% peptide.

Lipids and fluorophores were mixed in organic solvent after which the solvent was evaporated under a constant stream of N_2. The dry lipid film was hydrated in buffer (50 mM TRIS 140 mM NaCl, pH 7.4) at 60 ^{o}C and vortexed vigorously. The resulting multilamellar vesicles were then filtered 11 times through a polycarbonate filter with a pore size of 100 nm (Whatman International, Maidstone, UK) at 60 ^{o}C, resulting in LUVs with a diameter of approximately 100 nm. The quality of the formed LUVs was

verified with a Malvern Zetasizer Nano-S (Malvern Instruments, Worcestershire, UK). The percent of lipid incorporated into peptide containing LUVs was used as an indirect measure for the ability of the peptide to insert into the POPC bilayer.

Donor and acceptor LUVs were mixed 1:1 to a total lipid concentration of 80 μM. The samples were incubated for 72 hours at 37 ^{o}C to insure an equilibrium distribution of the labeled ceramide between donor and acceptor LUVs. The fluorescence lifetime of DPH-PC was measured at the 37 ^{o}C using a PicoQuant Fluotime 200 spectrometer (PicoQuant, Berlin, Germany) mounted with a 378 nm PDL 800-D pulsed diode laser and a PicoHarp event timer. In addition the lifetime of DPH-PC in the donor LUVs in the absence of acceptor LUVs (τ_{INI}) and the lifetime of DPH-PC in donor LUVs without ceramide-BODIPY (τ_0) were measured at the indicated temperature. The average lifetimes of all samples were calculated using the Fluofit software (PicoQuant).

From the time resolved data the FRET efficiency (*E*) was calculated for all samples according to

$$E = 1 - \frac{\tau_i}{\tau_0} \qquad [1]$$

As the FRET efficiency has a linear dependence on the concentration of ceramide-BODIPY in the donor LUVs, the fraction of ceramide-BODIPY in the donor LUVs (X_D) could be calculated from the FRET efficiency using the following equation (assuming that E is 0 upon total removal of ceramide-BODIPY from the donor LUVs)

$$X_D = \frac{E_{INI} - E_i}{E_{INI}} \qquad [2]$$

where E_{INI} is the FRET efficiency without transfer (with donor LUVs only) and E_i is the FRET efficiency in the particular mixture of donor and acceptor LUVs. When the molar fractions of ceramide-BODIPY in donor and acceptor LUVs are known, the partitioning coefficient (K) can be calculated according to

$$K = \frac{X_A C_A}{X_D C_D} \qquad [3]$$

where X_A and X_D are the molar fraction of ceramide in the acceptor and donor LUVs and C_A and C_D are the concentration of acceptor and donor LUVs.

Leucine uptake into cells

Cells were washed with Na^+-free EBSS (125 mM Choline chloride, 4.8 mM KCl, 1.2 mM $MgSO_4$, 1.2 mM KH_2PO_4, 1.3 mM $CaCl_2$, 5.6 mM Glucose, 25 mM HEPES, pH7.3) and were then incubated for two minutes at 37 ^{o}C with Na^+-free EBSS supplemented with 0.8 μCi/ml [^{3}H]-leucine. The cells were transferred to ice and washed three times with buffer. The cells were scraped in PBS containing 1% NP40. 2 x 5 μl lysate was set aside for protein determination and radioactivity was measured from the

remainder of the sample. The leucine uptake was corrected according to the protein content of the sample.

Leucine uptake into lysosomes

Leucine lysosomal uptake measurements were modified from previous studies[9,10]. Briefly, $4*10^6$ A431 cells, stably expressing WT or mutant LAPTM4B, were seeded in 150-mm cell culture dishes (one dish/sample). On the second day, cells were transfected with LAMP1-mGFP by using X-tremeGENE HP DNA transfection reagent (Sigma, Cat#06366236001) according to the manufacturer's instructions. 48 hours after transfection, cells were starved for amino acids in EBSS for 1 hour, then stimulated with EBSS-containing MEM amino acids, and 8 µL [^{3}H]-Leu (1 mCi/mL) for 10 minutes (10 mL stimulation mix/dish). The cells were then washed with cold PBS, scraped with 1 mL fractionation buffer (50 mM Kcl, 90 mM K-Gluconate, 1 mM EGTA, 5 mM $MgCl_2$, 50 mM Sucrose, 20 mM HEPES, pH 7.4 containing protease inhibitor cocktail), and finally mechanically broken by passing through a 23G needle (5 – 6 times) attached to a 1-mL syringe. Low-binding 1.5 mL tubes were used for all subsequent centrifugations. Lysates were centrifuged at 2,000 x g for 10 minutes at 4 ^oC. The post-nuclear supernatant (SNP) was further centrifuged at 17,000 x g for 30 minutes at 4 ^oC using a table top microcentrifuge. The subcellular fraction (pellet) containing lysosomes was carefully resuspended in 1 mL fractionation buffer and divided into two 1.5 mL tubes, each containing 25 µL pre-washed magnetic GFP-Trap®_MA beads. LAMP1-mGFP-specific lysosomes were pulled down by rotating the samples for 1 hour at 4 ^oC. After the pulldown, GFP-TRAP®_MA beads were washed two times with 1 mL cold fractionation buffer using a magnetic rack. LAMP1-mGFP-specific lysosomes were eluted with 50 µL SDS sample buffer per tube resulting in 100 µL of total eluate per sample. 10% of each sample were used for determining the total amount of protein for normalization. The remaining 90% of each sample were used for measuring the radioactivity by scintillation counting. Counts were normalized to total pulled down protein as the final measure of leucine lysosomal uptake.

Atomistic simulations

Peptide structure generation: The WALP23, LAPTM4B-TM3, LAPTM4B-TM3 D202A and LAPTM4B-TM4 peptides were created from their sequences (See **Figure S1**) using the Open Babel software. The generated peptides were acetylated and amidated in their N- and C-terminal domains using the Avogadro software. The resulting peptides were then forced to establish a perfect alpha helix structure by restraining their phi and psi dihedral angles to -64 and -41 degrees during a molecular dynamics

simulation of the peptides in the vacuum using force constant for these dihedrals of 1000 kJ mol^{-1} rad^{-2}.

Systems description: A full list of the systems simulated in this work can be found in **Tables S1-S3**. All systems share a lipid bilayer constituted of 512 POPC lipids. Each bilayer is hydrated using the recommended TIP3P water model including Van der Waals in hydrogens with 40 to 60 water molecules per lipid (**see Tables S1-S3**). Finally, we introduced Na^+ Cl^- ions to neutralize any excess of charge and set the aqueous phase to a physiologically relevant salt concentration (150 mmol of Na^+ Cl^-).

The differences between systems arise only from two main parameters; 1) the presence or absence of 10 transmembrane peptides (WALP23, LAPTM4B-TM3, LAPTM4B-TM3 D202A and LAPTM4B-TM4), and 2) the absence or presence of C16-ceramide molecules. In the latter case, the ceramides are initially either in the water phase (nine C16-Ceramides) or incorporated directly into the membrane randomly and symmetrically (50 [8 mol%] or 128 [20 mol%] C16-Ceramides).

Systems preparation and equilibration: The lipid only membrane systems have been prepared integrally using CHARMM-GUI [11]. These systems are the base of the protein containing systems. In brief, we have replicated the same peptide ten times and separated each peptide by a simple translation in the bilayer plane. From the 10 peptides, 5 where flipped, to create a system with 5 peptides C-terminus pointing up and 5 peptides N-terminus pointing up. Then, we have merged this system with the desired membrane as described in [12]. During this process, the peptides remain frozen. After the successful insertion we equilibrate the system further using NPT (1 bar, 310 K) molecular dynamics simulations. In these simulations, we restrain not only the backbone dihedrals as discussed above but also the relative position of the peptides by applying a linear bias potential with force constant of -500 KJ/mol between the center of mass of the peptides. This last potential maximizes the inter-peptide distance prior the production runs. This process depending on the system lasted between 100 and 200 ns until the inter-peptide distance was stable and the area per molecule fluctuated around a defined average value. Finally, we performed a short equilibration simulation (20 ns) without any constraint prior the production runs. Other simulation parameters of the equilibration, not explicitly given here, are equal to those in the production runs described below.

Production runs: All simulated systems use Gromacs 5.1.X or 2016 [13] using the charmm36 force field for the lipids (POPC and C16-ceramide) [14] and peptides (WALP23, LAPTM4B-TM3, LAPTM4B-TM3 D202A, and LAPTM4B-TM4) [15]. Few force field parameters missing for C16-ceramide were obtained from the CHARMMGUI [11]. Ions and water models used are the recommended ones by the force field. All simulations used a time step of 2 fs, and the total simulation length varied between 1 to 2 microseconds per run. In most of the cases, several replicas of each system were generated. The total

amount of simulation time of the project exceeds 70 microseconds. Simulation parameters used here are as provided by the CHARMM-GUI [11]. In brief, the NPT ensemble was provided by the Parrinello–Rahman barostat [16] and the Nóse–Hoover thermostat [17,18]. The time constants were set to 5 and 1 ps for the barostat and thermostat, respectively. The smooth PME scheme [19] was employed for electrostatics. The LJ interactions were cut off at 1.2 nm and the force switch modifier was employed from 1.0 nm on. The Verlet-type neighbor list was employed. The bonds connected to hydrogen atoms were constrained with the LINCS algorithm [20].

Co-immunoprecipitation and mass spectrometry

The identification of LAPTM4B interaction partners was carried out by Reversible Cross-Link Immuno-Precipitation (ReCLIP) [21]. Tandem Affinity Purification (TAP) was used to purify protein complexes followed by label-free protein quantitation with Mass Spectrometry. Briefly, single A431 clones overexpressing LAPTM4B or CD63 (as a negative control) with N-terminal 6His-Xpress and C-terminal 3XFlag tags were used [1]. Cells were cultured in complete medium or serum-free medium overnight. Cells were crosslinked in vivo with 0.4 mM DTME (Thermo Scientific; #22335) and 0.1 mM LC-SPDP (Thermo Scientific; #21651) in DPBS (PBS containing 0.5 mM $MgCl_2$ and 0.9 mM $CaCl_2$) for 2 hours on ice and quenched with 20 mM Tris-Cl (pH 8.0) and 5 mM DL-cysteine in DPBS for 15 minutes on ice. Crosslinked cells were lysed in lysis buffer buffer (50 mM Na_3PO_4, 0.3 M NaCl, 1% Triton X-100, pH 8.0) containing 6 M Urea and 5 mM Imidazole. Cell lysates were clarified by centrifuge at 16,000 x g for 15 minutes at 4 ^oC. The first purification step of LAPTM4B and CD63 was carried out by incubating cleared lysates with HIS-Select Nickel Affinity Gel (Sigma; P6611) for 1 hour at 4 ^oC, which was then washed twice with lysis buffer containing 6 M Urea and 10 mM Imidazole, and once with lysis buffer. Protein complexes were eluted with lysis buffer containing 250 mM Imidazole. The second purification was carried out by incubating the eluates from the first step with anti-Flag M2 Affinity gel (Sigma) for 2 hours at 4 ^oC. After binding, resins were washed three times with lysis buffer, once with 20 mM Tris-Cl (pH 8.0) containing 1% Triton X-100, and finally precipitated proteins were eluted with 0.05% formic acid. The eluates were concentrated by evaporation at 60 ^oC under vacuum with Thermo Savant DNA 110 SpeedVac, dissolved in 2x SDS buffer, and boiled for 30 minutes at 65 ^oC. Precipitated proteins were finally resolved by SDS-PAGE and followed by label-free protein quantitation using MS (Proteomics Unit, Institute of Biotechnology, University of Helsinki).

Statistical analysis

All the data are presented as the mean ± standard error of mean (SEM) from at least three independent experiments. Statistical significance was calculated using the Student's t-test. The level of statistical significance was set at 0.05 for all the tests.

(1) Blom, T.; Li, S.; Dichlberger, A.; Bäck, N.; Kim, Y. A.; Loizides-Mangold, U.; Riezman, H.; Bittman, R.; Ikonen, E. LAPTM4B Facilitates Late Endosomal Ceramide Export to Control Cell Death Pathways. *Nat. Chem. Biol.* **2015**, *11*, 799–806.

(2) Hobbs, S.; Jitrapakdee, S.; Wallace, J. C. Development of a Bicistronic Vector Driven by the Human Polypeptide Chain Elongation Factor 1α Promoter for Creation of Stable Mammalian Cell Lines That Express Very High Levels of Recombinant Proteins. *Biochem. Biophys. Res. Commun.* **1998**, *252*, 368–372.

(3) Kuokkanen, E.; Smith, W.; Mäkinen, M.; Tuominen, H.; Puhka, M.; Jokitalo, E.; Duvet, S.; Berg, T.; Heikinheimo, P. Characterization and Subcellular Localization of Human Neutral Class II Alpha-Mannosidase [Corrected]. *Glycobiology* **2007**, *17*, 1084–1093.

(4) Falcon-Perez, J. M.; Nazarian, R.; Sabatti, C.; Dell'Angelica, E. C. Distribution and Dynamics of Lamp1-Containing Endocytic Organelles in Fibroblasts Deficient in BLOC-3. *J. Cell Sci.* **2005**, *118*, 5243–5255.

(5) Salo, V. T.; Belevich, I.; Li, S.; Karhinen, L.; Vihinen, H.; Vigouroux, C.; Magré, J.; Thiele, C.; Hölttä-Vuori, M.; Jokitalo, E.; *et al.* Seipin Regulates ER-Lipid Droplet Contacts and Cargo Delivery. *EMBO J.* **2016**, *35*, 2699–2716.

(6) Ran, F. A.; Hsu, P. D.; Wright, J.; Agarwala, V.; Scott, D. A.; Zhang, F. Genome Engineering Using the CRISPR-Cas9 System. *Nat. Protoc.* **2013**, *8*, 2281–2308.

(7) Pietiäinen, V.; Vassilev, B.; Blom, T.; Wang, W.; Nelson, J.; Bittman, R.; Bäck, N.; Zelcer, N.; Ikonen, E.; Pietiainen, V.; *et al.* NDRG1 Functions in LDL Receptor Trafficking by Regulating Endosomal Recycling and Degradation. *J. Cell Sci.* **2013**, *126*, 3961–3971.

(8) Ijäs, H. K.; Lönnfors, M.; Nyholm, T. K. M. M. Sterol Affinity for Phospholipid Bilayers Is Influenced by Hydrophobic Matching between Lipids and Transmembrane Peptides. *Biochim. Biophys. Acta - Biomembr.* **2013**, *1828*, 932–937.

(9) Milkereit, R.; Persaud, A.; Vanoaica, L.; Guetg, A.; Verrey, F.; Rotin, D. LAPTM4b Recruits the LAT1-4F2hc Leu Transporter to Lysosomes and Promotes mTORC1 Activation. *Nat. Commun.* **2015**, *6*, 7250.

(10) Zoncu, R.; Bar-Peled, L.; Efeyan, A.; Wang, S.; Sancak, Y.; Sabatini, D. M. mTORC1 Senses Lysosomal Amino Acids through an inside-out Mechanism That Requires the Vacuolar H(+)-ATPase. *Science* **2011**, *334*, 678–683.

(11) Lee, J.; Cheng, X.; Swails, J. M.; Yeom, M. S.; Eastman, P. K.; Lemkul, J. A.; Wei, S.; Buckner, J.; Jeong, J. C.; Qi, Y.; *et al.* CHARMM-GUI Input Generator for NAMD, GROMACS, AMBER, OpenMM, and CHARMM/OpenMM Simulations Using the CHARMM36 Additive Force Field. *J. Chem. Theory Comput.* **2016**, *12*, 405–413.

(12) Javanainen, M. Universal Method for Embedding Proteins into Complex Lipid Bilayers for Molecular Dynamics Simulations. *J. Chem. Theory Comput.* **2014**, *10*, 2577–2582.

(13) Abraham, M. J.; Murtola, T.; Schulz, R.; Páll, S.; Smith, J. C.; Hess, B.; Lindahl, E. GROMACS: High Performance Molecular Simulations through Multi-Level Parallelism from Laptops to Supercomputers. *SoftwareX* **2015**, *1-2*, 19–25.

(14) Klauda, J. B.; Venable, R. M.; Freites, J. A.; O'Connor, J. W.; Tobias, D. J.; Mondragon-Ramirez, C.; Vorobyov, I.; MacKerell, A. D.; Pastor, R. W. Update of the CHARMM All-Atom Additive Force Field for Lipids: Validation on Six Lipid Types. *J. Phys. Chem. B* **2010**, *114*, 7830–7843.

(15) Huang, J.; MacKerell, A. D. CHARMM36 All-Atom Additive Protein Force Field: Validation Based on Comparison to NMR Data. *J. Comput. Chem.* **2013**, *34*, 2135–2145.

(16) Parrinello, M.; Rahman, A. Polymorphic Transitions in Single Crystals: A New Molecular Dynamics Method. *J. Appl. Phys.* **1981**, *52*, 7182–7190.

(17) Nosé, S. A Unified Formulation of the Constant Temperature Molecular Dynamics Methods. *J. Chem. Phys.* **1984**, *81*, 511–519.

(18) Hoover. Canonical Dynamics: Equilibrium Phase-Space Distributions. *Phys. Rev. A, Gen. Phys.* **1985**, *31*, 1695–1697.

(19) Essmann, U.; Perera, L.; Berkowitz, M. L.; Darden, T.; Lee, H.; Pedersen, L. G. A Smooth Particle Mesh Ewald Method. *J. Chem. Phys.* **1995**, *103*, 8577–8593.

(20) Hess, B.; Bekker, H.; Berendsen, H. J. C.; Fraaije, J. G. E. M. LINCS: A Linear Constraint Solver for Molecular Simulations. *J. Comput. Chem.* **1997**, *18*, 1463–1472.

(21) Smith, A. L.; Friedman, D. B.; Yu, H.; Carnahan, R. H.; Reynolds, A. B. ReCLIP (Reversible Cross-Link Immuno-Precipitation): An Efficient Method for Interrogation of Labile Protein Complexes. *PLoS One* **2011**, *6*, e16206.

(22) Bandhuvula, P.; Li, Z.; Bittman, R.; Saba, J. D. Sphingosine 1-Phosphate Lyase Enzyme Assay Using a BODIPY-Labeled Substrate. *Biochem. Biophys. Res. Commun.* **2009**, *380*, 366–370.

(23) Lu, X.; Cseh, S.; Byun, H.-S.; Tigyi, G.; Bittman, R. Total Synthesis of Two Photoactivatable Analogues of the Growth-Factor-like Mediator Sphingosine 1-Phosphate: Differential Interaction with Protein Targets. *J. Org. Chem.* **2003**, *68*, 7046–7050.

Figure S1.

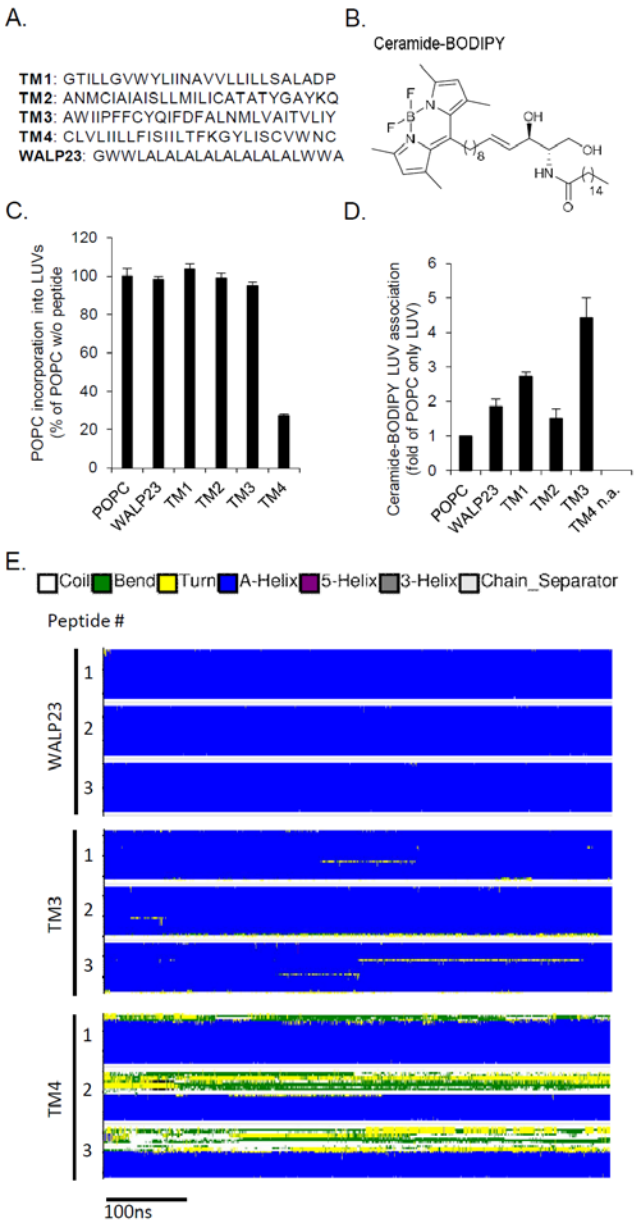

Figure S1. Behavior of LAPTM4B transmembrane domain peptides in LUVs.

(A) Sequences of the transmembrane peptides used in the lipid transfer assay are shown. For the LAPTM4B peptides (TM1, TM2, TM3, and TM4), the predicted membrane embedded segment plus 2 residues at each terminal were synthesized. WALP23 was used as a control peptide. (B) Chemical structure of Ceramide-BODIPY [1,22] used as a probe in the lipid transfer assay. (C) Formation of LUVs with or without TM peptides. The incorporation efficiency of TM peptides into LUVs is shown. TM4-containing LUVs were inefficiently formed, suggestive of membrane disrupting properties of the peptide. Values represent mean ± SEM of three experiments. (D) The association of Ceramide-BODIPY with LAPTM4B-TM-containing LUVs was studied by a FRET-based in vitro lipid transfer assay. Values represent mean ± SEM of three experiments. TM4 was not analyzed (see Figure S1C). (E) Temporal evolution of the secondary structure of the studied transmembrane peptides in atomistic simulations. TM4 alpha helical imposed initial structure is not stable contrary to TM3 and WALP23. Three representative examples are shown for each peptide.

Figure S2.

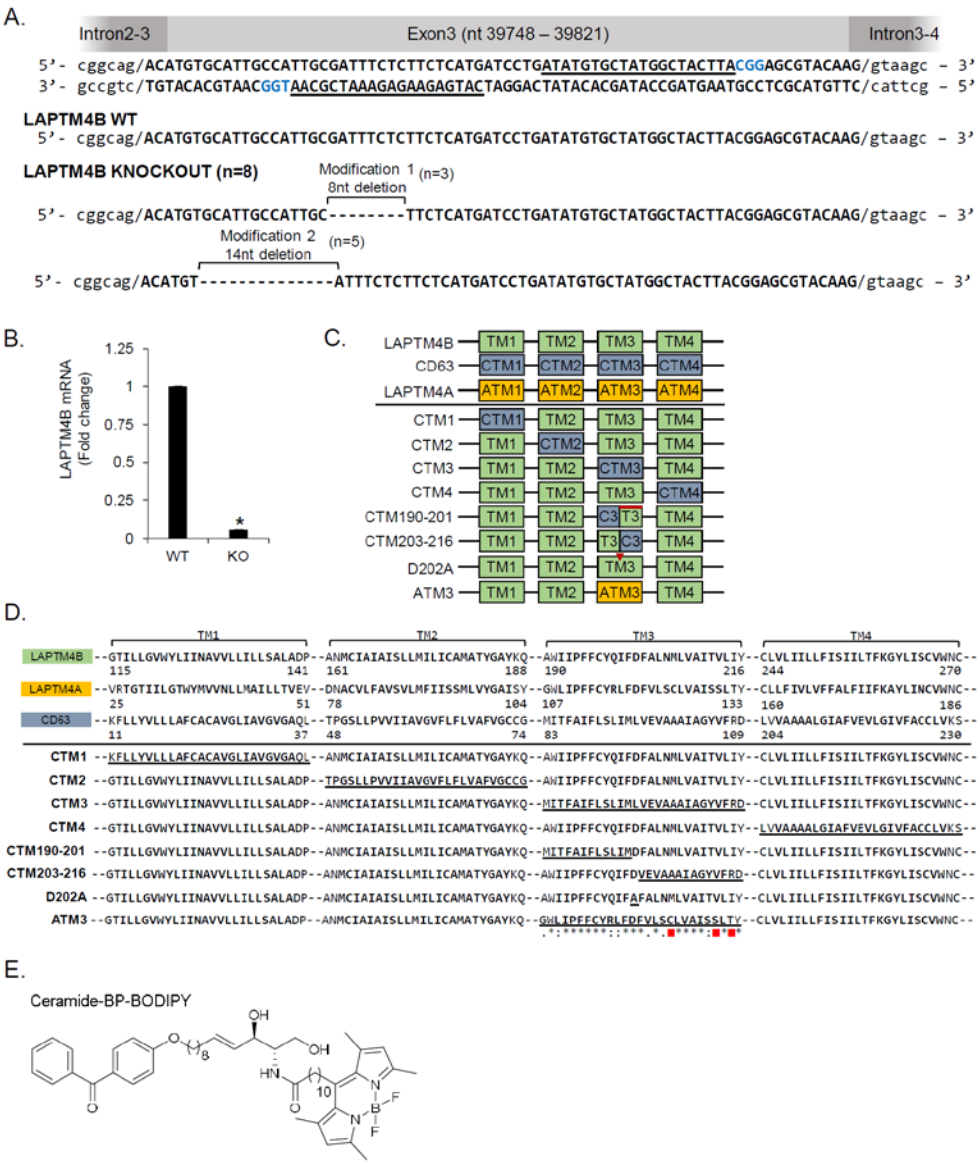

Figure S2. Genomic modifications of LAPTM4B knockout, wild type, and mutant cell lines.

(A) CRISPR/Cas9 target site sequences in LAPTM4B are underlined. Genomic LAPTM4B modifications in A431 LAPTM4B knockout cells were verified by sequencing. The number of sequenced clones is indicated. (B) LAPTM4B transcript levels in A431 LAPTM4B knockout and WT cells were assessed by qPCR. All values represent mean ± SEM of three experiments and differences are significant for $p^* < 0.05$. (C) Schematic representation of LAPTM4B WT and mutant constructs that were used for generating stable A431 cell lines on a LAPTM4B knockout background. CD63 and LAPTM4A were used as controls. All cell lines used in this study are named accordingly to the construct name. The individual TM domains are depicted as boxes, the sphingolipid binding motif is marked by a red line, and the D202A mutation is indicated by a red arrow head. (D) Amino acid sequences of LAPTM4B WT, LAPTM4B mutants, CD63, and LAPTM4A are shown. Underlined sequences indicate the detailed modifications in LAPTM4B and correspond to the schematic representation shown in (C). The red squares show the non-conserved residues in ATM3 compared to wild type LAPTM4B. The asterisks (*) denote identical residues, colon (:) indicates amino acid residues with strongly similar properties and period (.) show residues with similar properties in ATM3 compared to LAPTM4B. (E) Chemical structure of the crosslinkable probe Ceramide-BP-BODIPY [1,23] that was used to assess ceramide protein interactions.

Figure S3.

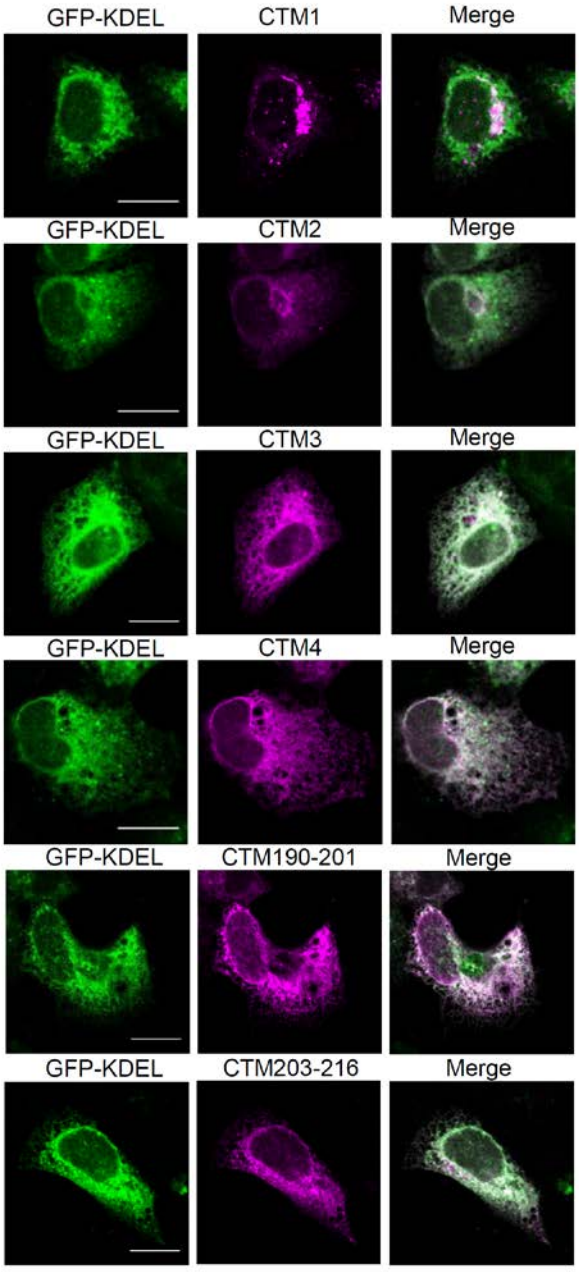

Figure S3. Cellular localization of the LAPTM4B mutant constructs.
Cells stably expressing 3xFlag-tagged LAPTM4B mutant proteins (CTM1, CTM2, CTM3, CTM4, CTM190-201, or CTM203-216) were transfected with the ER marker GFP-KDEL and the proteins were assessed for colocalization. Scale bar 20µm.

Figure S4.

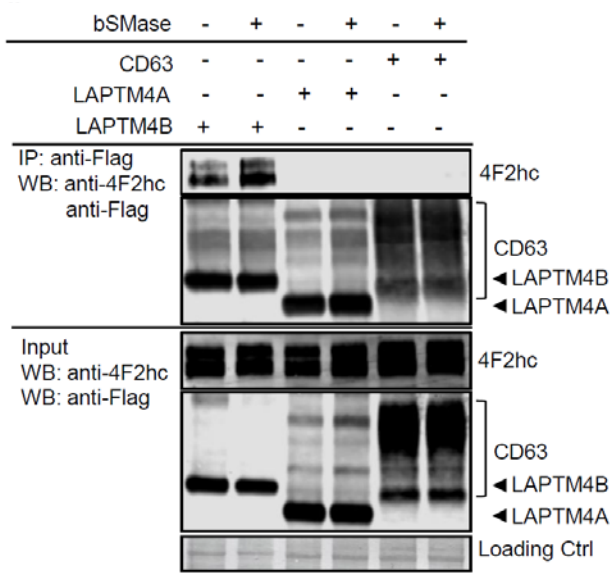

Figure S4. Interaction of endogenous 4F2hc with LAPTM4B and control proteins.
A431 cells stably expressing 3xFLAG-tagged LAPTM4B, CD63, or LAPTM4A cells were treated with bSMase (50mU/mL, 30 min) and the interaction of LAPTM4B, CD63, and LAPTM4A with endogenous 4F2hc was assessed by Co-immunoprecipitation followed by Western blotting. Three independent experiments have been performed and one representative experiment is shown.

Figure S5.

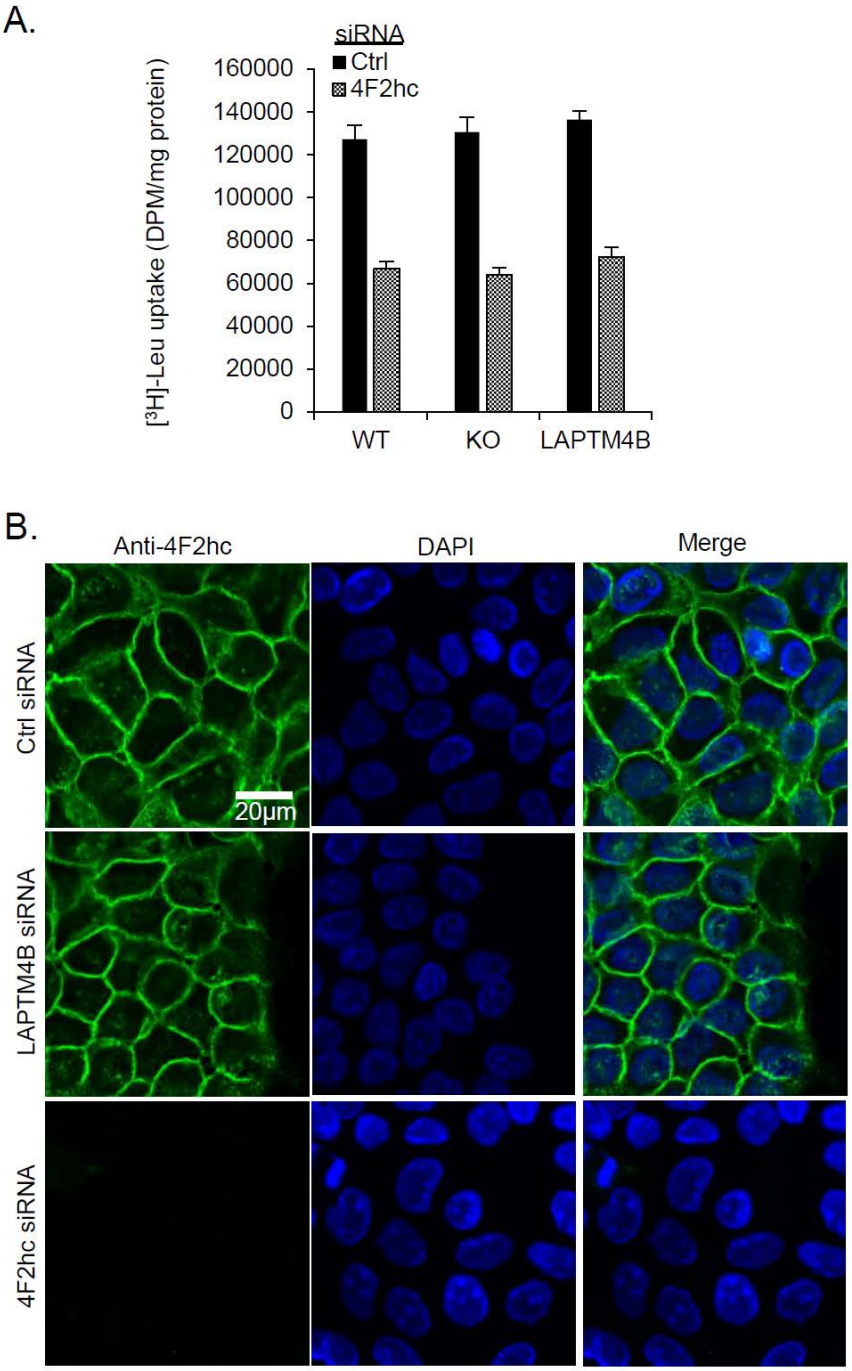

Figure S5. LAPTM4B does not affect 4F2hc-dependent leucine uptake into cells.
(A) 4F2hc-silenced A431 WT, LAPTM4B knockout, and LAPTM4B overexpressing cells were washed in Na^+-free EBSS and cellular uptake of [^{3}H]-leucine (0.8 µCi/mL in Na^+-free EBSS) during 2 minutes was measured by scintillation counting. (B) Expression and cellular localization of 4F2hc in control cells and in cells depleted of LAPTM4B or 4F2hc. The majority of 4F2hc is localized to the plasma membrane in both control and LAPTM4B depleted cells. Scale bar 20µm.

Figure S6.

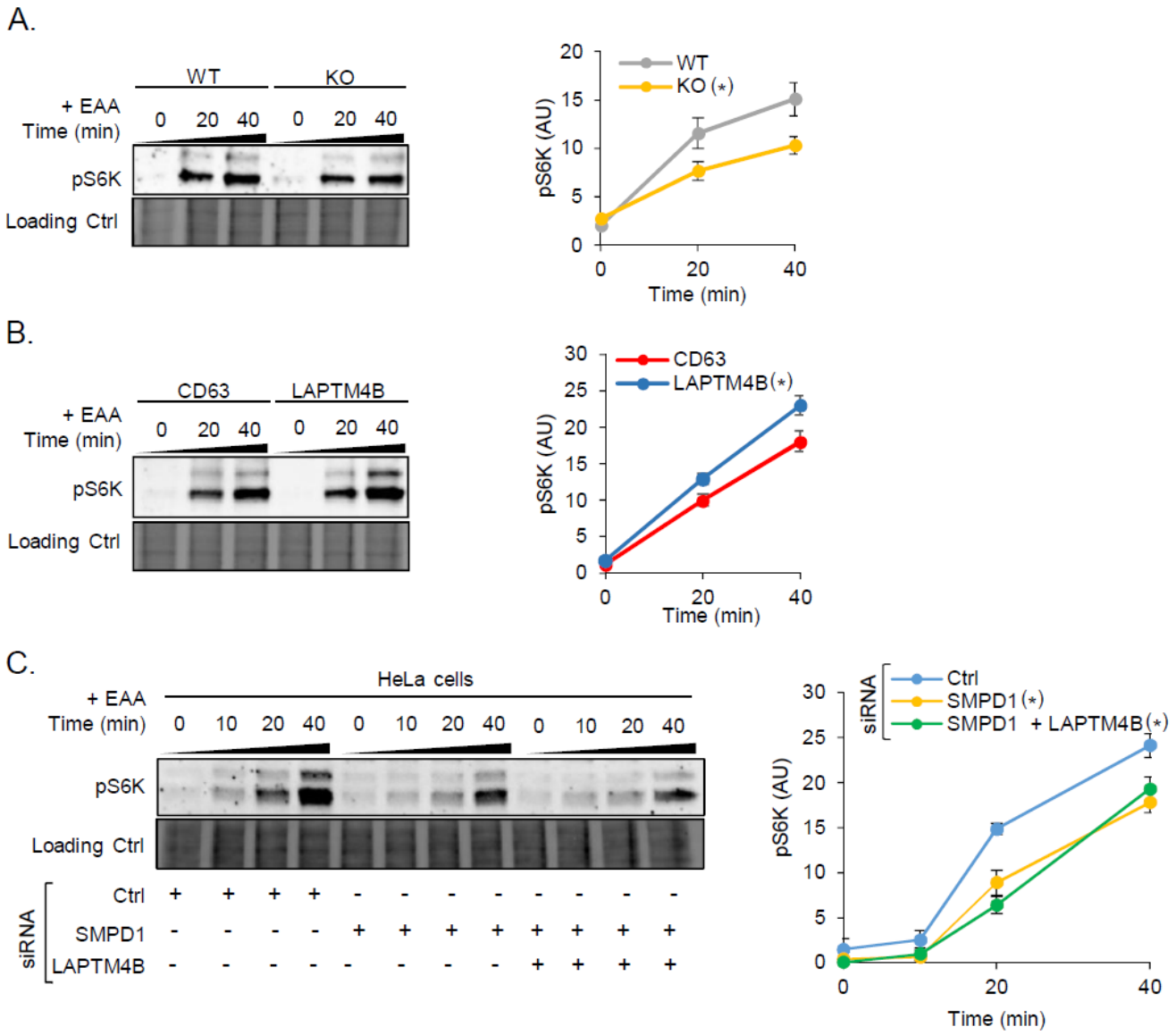

Figure S6. LAPTM4B affects mTORC1 activity.
(A) A431 WT and LAPTM4B knockout cells, or (B) A431 CD63 and LAPTM4B cells were starved (1 h with EBSS), and pS6K expression was assessed by Western blotting upon refeeding with stimulation medium for the indicated time points. Left panels: representative experiments; right panels: quantification of n = 3 experiments, mean ± SEM, differences are significant for p* < 0.05 compared to control. (C) SMPD1- or/and LAPTM4B-silenced Hela cells were starved (1 h with EBSS), and pS6K expression was assessed by Western blotting upon refeeding upon refeeding with stimulation medium for the indicated time points. Left panel: representative experiment; right panel: quantification of n = 3 experiments, mean ± SEM, differences are significant for p* < 0.05 compared to control.

Figure S7.

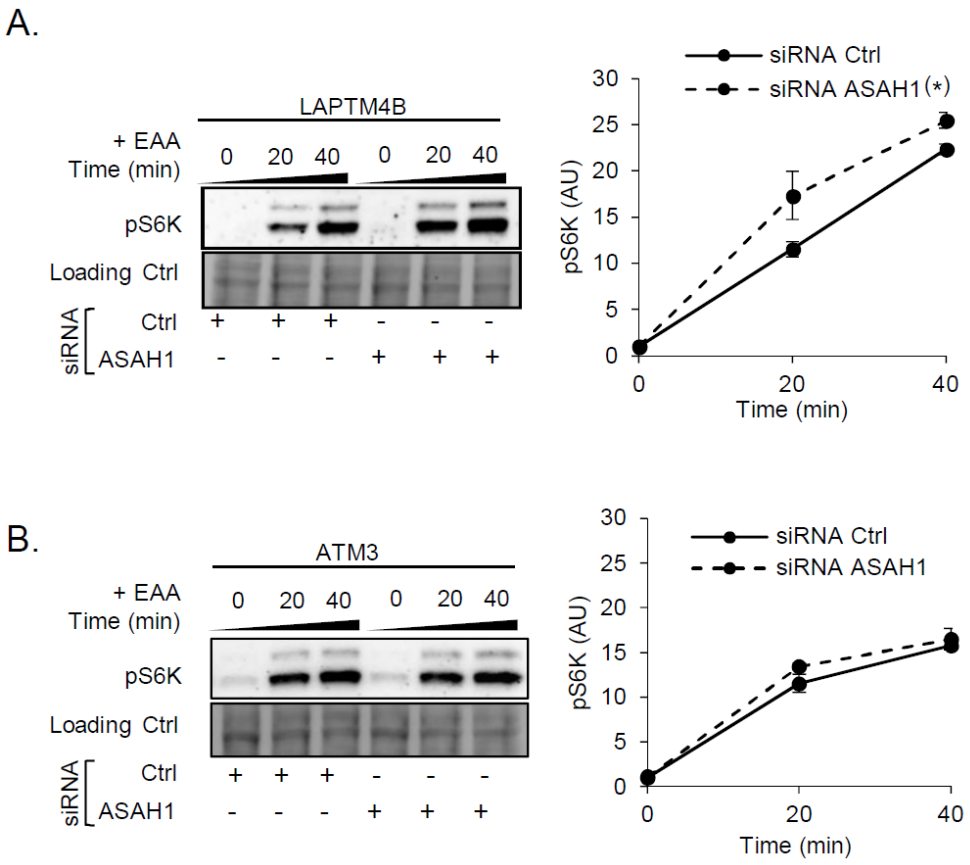

Figure S7. The interaction of ceramide with LAPTM4B affects mTORC1 activity.
(A) Control- or ASAH1-silenced LAPTM4B, or (B) ATM3 mutant cells were starved (1 h with EBSS), and pS6K expression was assessed by Western blotting upon refeeding with stimulation medium for the indicated time points. Left panels: representative experiments; right panels: quantifications of n = 3 experiments, mean ± SEM, differences are significant for p* < 0.05 compared to control.

Additional supporting information:

Tables S1-S3. Description of the simulated systems

Tables S4-S9. Fundamental properties of the simulated membranes, and their incorporation of micellar ceramide

Table S10. Full results of the proteomic screen

Tables S11-13. List of used DNA constructs, oligos and siRNAs

Movie S1.Entry of micellar ceramide into a TM3-containing POPC membrane